Effect of Surface Morphologies and Chemistry of Paper on Deposited Collagen

Boyce S. Chang,[1,2] Anuraag Boddupalli,[3] Andrea F. Boyer,[4] Millicent Orondo,[1] Jean-Francis Bloch,[5] Kaitlin M. Bratlie,[1,2,3] Martin M. Thuo,[1,6,7*]*

[1]Department of Materials Science & Engineering, Iowa State University, Ames, Iowa 50011, USA

[2]Division of Materials Sciences and Engineering, Ames National Laboratory, Ames, Iowa 50011, USA

[3]Department of Chemical & Biological Engineering, Iowa State University, Ames, Iowa 50011, USA

[4]Department of Mechanical Engineering, Iowa State University, Ames, Iowa 50011, USA

[5]Institute of Engineering, Université Grenoble Alpes, 3SR, F-38000 Grenoble, France

[6]Department of Electrical & Computer Engineering, Iowa State University, Ames, Iowa 50011, USA

[7]Center for Crop Utilization Research, Iowa State University, Ames, Iowa 50011, USA

CORRESPONDING AUTHOR FOOTNOTE

[*]To whom correspondence should be addressed: E-mail: mthuo@iastate.edu, kbratlie@iastate.edu

Abstract

Paper-based platforms for biological studies have received significant attention given that cellulose is ubiquitous, biocompatible, and can be readily organized into tunable fibrous structures. In the latter form, effect of complexity in surface morphologies (roughness, porosity and fiber organization) on cell-substrate interaction have not been thoroughly explored. We infer that altering the properties of a fibrous material should lead to significant changes in cellular microenvironment and direct the deposition of structurally analogous extracellular matrix (fiber-fiber templating) like collagen. Here, we elucidate the effect of varying paper roughness and surface chemistry on NIH/3T3 fibroblasts via organization of excreted collagen. Collagen intensity was found to increase linearly with paper porosity, indicating a 3D culture platform. The intensity, however, decays over time due to biodegradation of the substrate. Stability can be improved by introducing fluorinated alkyl silanes to yield hydrophobic paper. This process concomitantly transforms the substrate to a 2D-like scaffold where collagen is predominantly assembled on the surface, thus changing the cellular microenvironment. Altering surface energy also led to fluctuations in collagen intensity and organization over time for smooth (calendered) paper substrates. We infer that the increased roughness improves collagen adsorption through capillary driven petal effect. In general, the influence of the substrate simultaneously affects its ability to host collagen and guide orientation. These findings offer insights into the effects of secondary structures and chemistry of fibrous polymeric materials on cell culture, which we propose as vital parameters when using paper-based platforms.

1. Introduction

Cellulose is widely regarded as an important biopolymer due to its biocompatibility, porosity, tunable chemistry and abundance.[1] Post extraction, modification and processing of the polymer has led to myriad of applications over eons of human civilization.[2] This plant-derived polymer, typically supports nutrient transport through a combination of pore structure and surface chemistry.[3] For these reasons, cellulose has emerged as an attractive material for cell or bio-based studies.[4, 5] Recent reports on the application of cellulose as a substrate for cell culture have largely focused on the effects of microstructure, which depends on the source of the material.[4, 6, 7] In practice, however, cellulose is used in the form of bulk fibrous materials like paper[8, 9] whereby 'secondary structures' such as fiber organization, porosity, surface roughness, surface energy, and/or additives could also dictate performance.

The effects of these so-called secondary structures on extracellular matrix and cellular responses have not been widely explored. The lack of literature, despite emerging interest of paper as a substrate for biological studies, is complicated by the multi-scale nature of such studies and challenges in isolating contributions from each parameter. Furthermore, the structure of paper is supported by secondary bonds between cellulose fibers and is therefore susceptible to degradation when used for biological studies.[10] Solutions used to mitigate this drawback often utilize hydrophobic coatings such as polyperfluorodecyl acrylate (pPFDA) to improve stability.[11, 12] We and others have recently demonstrated that tuning the surface chemistry of paper could result in templated synthesis of materials and conductive networks, among others.[13, 14] However, the effects of surface energy on cell-matrix interaction in paper have not been thoroughly examined.

Herein, we aim to investigate the effects of secondary structures—specifically, the role of surface roughness, porosity and chemistry—on cell-substrate interactions, hence the intensity and

degree of order in deposited extracellular matrix (ECM). When the latter is collagen, organization of the deposited fiber bundles can be captured spectroscopically.[15] Paper substrates were fabricated in-house to ensure control over the secondary structure of paper, allowing us to isolate the effect of roughness and porosity by tuning the level of calendering. Furthermore, surface chemistry can be modified without significantly altering the physical morphology through surface step-growth polymerization between alkyl silanes and physisorbed water,[16, 17] which allows us to decouple the effects of structure and surface chemistry. Note that "surface" refers to cellulose-culture media interface, which includes both exposed and buried fibers. As a model system, we selected NIH/3T3 fibroblast cells cultured on paper fabricated using lignin-free bleached softwood kraft pulp. Changes in the secondary structure of paper after calendering (**Figure 1a**),[18, 19] is ascertained using X-ray tomography (**Figure 1b-c**). As expected, decrease in asymmetry of porosity (**Figure 1a**) is observed through densification upon calendaring and subsequent convergence of the pore structure (**Figure 1c**).

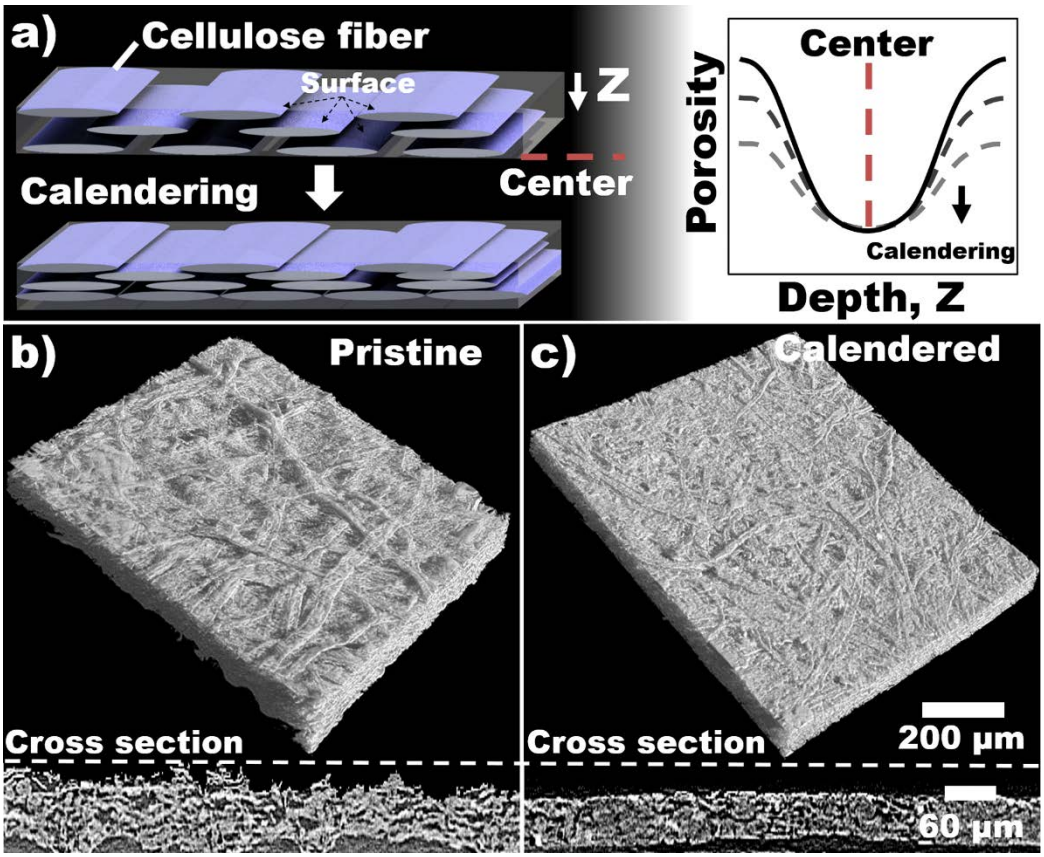

Figure 1. Tuning the complex surface porosity of paper: (a) Schematic of the calendering process capturing decrease in surface porosity with preserved fiber organization. X-ray tomography images of surface and associated cross-section of (b) as-formed and (c) calendered paper illustrating retention of fiber order on the surface and increased smoothness.

2. Materials and Methods

All papers were custom prepared as described below. Trichloro(1H, 1H, 2H, 2H-perfluorooctyl)silane was purchased from Sigma-Aldrich (Milwaukee, WI) and used as supplied. Phosphate buffered saline (PBS) (Fisher Scientific, Pittsburgh, PA) were used as supplied. NIH/3T3 mouse fibroblasts were purchased from ATCC (Manassas, VA).

2.1 Paper fabrication

The paper substrates were fabricated at the Center for Paper Technology (CTP, Grenoble, France) and were based on bleached softwood kraft pulp refined with hydrafiner at SR-25, sized with 1.5% Pescol glue at a pH 4.5. The sheets were manufactured on a dynamic sheet former with a constant web speed of 80 $m.min^{-1}$ for 5 minutes. Jet and fabric speed differences were set between -30 and +30 $m.min^{-1}$. The basis weight was measured to be *ca* 49 $g{\cdot}m^{-2}$. Differences in jet and wire (mesh) velocities (V_{jet}-V_{wire} = -5.7 m/min) led to a shear driven bias in fiber orientation (Table 1). The average fiber orientation was ~48° implying a slight bias towards the machine directions (direction of flow, abbreviated MD) relative to the cross direction (CD). To confirm this bias, a small percentage of dyed fibers were introduced to the pulp and the observed ratio of fibers orientation was CD:MD = 1:1.7 (Table 1). For clarity and brevity, we adopted a nomenclature based on the degree of calendaring. Paper I represent pristine substrate as prepared, paper II was calendered once at 45 $N.m^{-2}$ and paper III was calendered via repeated passing (10 times) through the rollers at 100 $N.m^{-2}$.

Table 1. Parameters applied for the fabrication of custom-made cellulose substrates.

Parameter	**Value**
V_{JET} - V_{Wire} ($m.min^{-1}$)	-5.7
Mean fiber orientation (0 = CD; 90° = MD), $\bar{\theta}_n$ (°)	47.6
Ratio of the number of fibers in the MD vs CD n_{MD} / n_{CD}	1.7

2.2 Surface treatment

The paper samples were cut (2 × 2 cm^2) and placed into a desiccator containing *ca.* 100 g of calcium sulfate desiccant (W.A. Hammond Drierite Co., LTD, Xenia, OH). A vial containing 100 μL of trichloro(1H, 1H, 2H, 2H-perfluorooctyl)silane (Sigma Aldrich, Milwaukee, WI) was

placed into the desiccator and the setup was evacuated to *ca.* 30 mmHg for 1 min and then placed in an oven (95°C for 5 h). Vacuum was gently released before removing the samples. Similarly treated microscope glass slides were prepared as non-porous surface chemistry controls.

2.3 Scanning electron microscopy (SEM)

Micrographs were obtained using an FEI Quanta 250 field emission SEM (FEI, Hillsboro, OR). Low pressure (80 Pa H_2O) mode was used to reduce charge build-up on the surface of the insulating cellulose substrate. The backscattered electron detector was used along with the following conditions: 10 kV accelerating voltage, 10 mm working distance, and frame integration was used to enhance signal to noise ratio.

2.4 Surface profilometry

Surface profiles were obtained using a Zygo NewView 7100 Optical surface profiler (Zygo, Middlefield, CT), coupled with a 5× objective lens. Due to the unevenness and undulations inherent to the cellulose substrates, a 150 µm scan length (depth) was used. Three areas were analyzed for each substrate. The scale was held constant between 40 and -40 µm. A 2D profile was obtained by taking a 2 mm diagonal across the scan area. A plane removal function was used to compensate for the tilt inherent in the substrate. Swedish height is defined by Zygo® to be the distance between 2 boundaries, the 10th and 95th percentile of the height population.

2.5 X-ray tomography

X-ray tomography was performed using a synchrotron source at the ESRF beamline ID 19, Grenoble, France.[20, 21]

2.6 Contact angle

Contact angle measurements on the silanized substrates were obtained using ramé-Hart Goniometer 100-00 (ramé-hart instrument, Lake Mountains, NJ) with a tilting base. Deionized

water was used as the probe liquid (1 µL) and was dispensed onto cellulose through an integrated syringe pump.

2.7 Cell culture

NIH/3T3 mouse fibroblasts (ATCC, Manassas, VA) were cultured at 37°C with 5% CO_2 in complete medium (CM, Dulbecco's modified Eagle's medium (Thermo Scientific, Waltham, MA) supplemented with 10% bovine calf serum (Sigma Aldrich, St. Louis, MO), 100 U/L penicillin and 100 $\mu g \cdot mL^{-1}$ streptomycin (Fisher Scientific, Pittsburgh, PA)). Cells were passaged every three days using 0.025% Trypsin-EDTA (Thermo Scientific) and sub-cultured at 1.3×10^4 $cells \cdot cm^{-2}$.

Samples and controls were washed twice with phosphate buffered saline (PBS) (Fisher Scientific) prior to immersion in 2 mL of CM. All the samples were seeded at 1.0×10^4 $cells \cdot cm^{-2}$ in 35 mm^2 Petri dishes. CM was renewed every three days. Samples were subsequently fixed using 10% buffered formalin (Fisher Scientific) for 20 min.

2.8 Polarized second harmonic generation (SHG) microscopy imaging

A mode-locked Ti:Sapphire laser system (100 fs pulse width, 1 kHz repetition rate, Libra, Coherent, Santa Clara, CA) that produced an 800 nm fundamental was used for SHG imaging. Average power at the microscope stage was controlled using a half-wave plate and a Glan-Thompson polarizer (Thorlabs, Newton, NJ), and maintained between 1 to 10 mW to avoid damage to the cells. SHG images were collected in transmission mode, using a setup that included an inverted microscope (AmScope, Irvine, CA) and a 20× Nikon Plan Fluorite objective (0.50 NA, 2.1 mm) to focus the fundamental. The signal was collected using a 40× Nikon water immersion objective (0.8 NA, 3.5 mm). A dichroic mirror was used to reflect the SHG signal. The signal was filtered using a short pass filter (<450 nm, Thorlabs) and an 808 nm notch filter (Melles Griot,

Rochester, NY). The signal was detected using an iCCD camera (iStar 334T, Andor, Belfast, UK) with 512 × 512 active pixels. Polarization of the SHG signal for imaging the samples was modulated using a Glan-Thompson polarizer and a half-wave plate mounted on a motor-driven rotational stage (Thorlabs). Images of the collagen signal from the samples were collected every 10° from 0 to 350°. A minimum of three sets of polarization images were collected for each experimental condition.

2.9 Image processing

The intensity of the second harmonic signal of collagen fiber as a function of polarization angle of the incident laser beam can be written as:

$$I_{SHG} = c.\left\{\left[(\sin(\theta_e - \theta_0))^2 + \left(\frac{\chi_{zzz}}{\chi_{zxx}}\right)(\cos(\theta_e - \theta_0))^2\right]^2 + \left(\frac{\chi_{xzx}}{\chi_{zxx}}\right)^2 (\sin(2(\theta_e - \theta_0)))^2\right\} \quad \text{Equation 1}$$

where $\left(\frac{\chi_{zzz}}{\chi_{zxx}}\right)$ and $\left(\frac{\chi_{xzx}}{\chi_{zxx}}\right)$ are second-order susceptibility tensor element ratios; θ_e and θ_0 are the incident polarization angle and collagen fiber angle, respectively; and c is a normalization constant. ImageJ (NIH, Bethesda, MD) was used to analyze the images which were binned to obtain regions of interest (ROIs) of 2 × 2 pixels. Collagen orientation angles were evaluated for each ROI by fitting the binned images to a Levenberg-Marquardt algorithm using Matlab (MathWorks, Natick, MA). A threshold of 5 counts per pixel was used to exclude ROIs from the analysis, as it is below the limit of detection for this setup. The MATLAB script generated images displaying the orientation angles of collagen determined for each ROI and histograms for each image.

2.10 DNA quantification

The amount of DNA in each sample was quantified using the Quant-It™ dsDNA High-Sensitivity Assay Kit (Fisher Scientific). Cells were lysed using 1000 µL of lysis buffer (Fisher Scientific) and placed on ice for 10 min. To each sample, 1.2 mL of RNase (15 mg·mL^{-1}) was

added and the samples were incubated at room temperature for 1 h. Working solution of the DNA reagent was prepared by diluting the high sensitivity (HS) reagent (1:200) in the HS buffer. Samples (10 µL) were added to 200 µL of the working solution and the plate was read at an excitation of 480 nm and an emission of 530 nm using a BioTek Synergy HT Multi-detection Microplate Reader (BioTek, Winooski, VT). The concentration of DNA was determined by comparing the absorbance to a standard curve of known DNA concentrations.

2.11 Statistical analysis

JMP® statistical software (Cary, NC) was used to analyze and compute the significant difference comparisons via a two-way ANOVA. Tukey's honest significance difference test was used to evaluate pair-wise comparisons. Differences were considered statistically significant for $p < 0.05$.

3. Background

Collagen is the most abundant structural protein in mammals,[22, 23] occurring primarily as ordered or disordered heterogeneous structures.[15, 24-27] Directing orientation in collagen is critical in the development of *in vitro* methods to generate implantable tissue. Collagen organization is not only important in tissue engineering due to effects on mechanical properties but also in prognosis.[28-32] Various *in vivo*[27, 28] and *in vitro*[15, 25] methods have been used to control degree of order in deposited collagen. Extracellular matrix deposition, however, depends on the nature of the environment on which the cells are cultured. The use of material surface characteristics to direct collagen deposition has been explored, and often requires sophisticated fabrication techniques or culture methods.[33-38]

More recently, scaffolds that mimic the fibrous environment found in tissues were used to improve fibroblast adhesion and proliferation.[39] Cellulose substrates, therefore, potentially serve as flexible materials for fabrication of low cost, versatile scaffolds for designing diverse biomedical applications.[40] The fabrication of such materials, however, often result in various bulk morphologies. Thus, it is crucial to identify the effects of such secondary structures on cellular interactions in order to transition towards widespread applications.

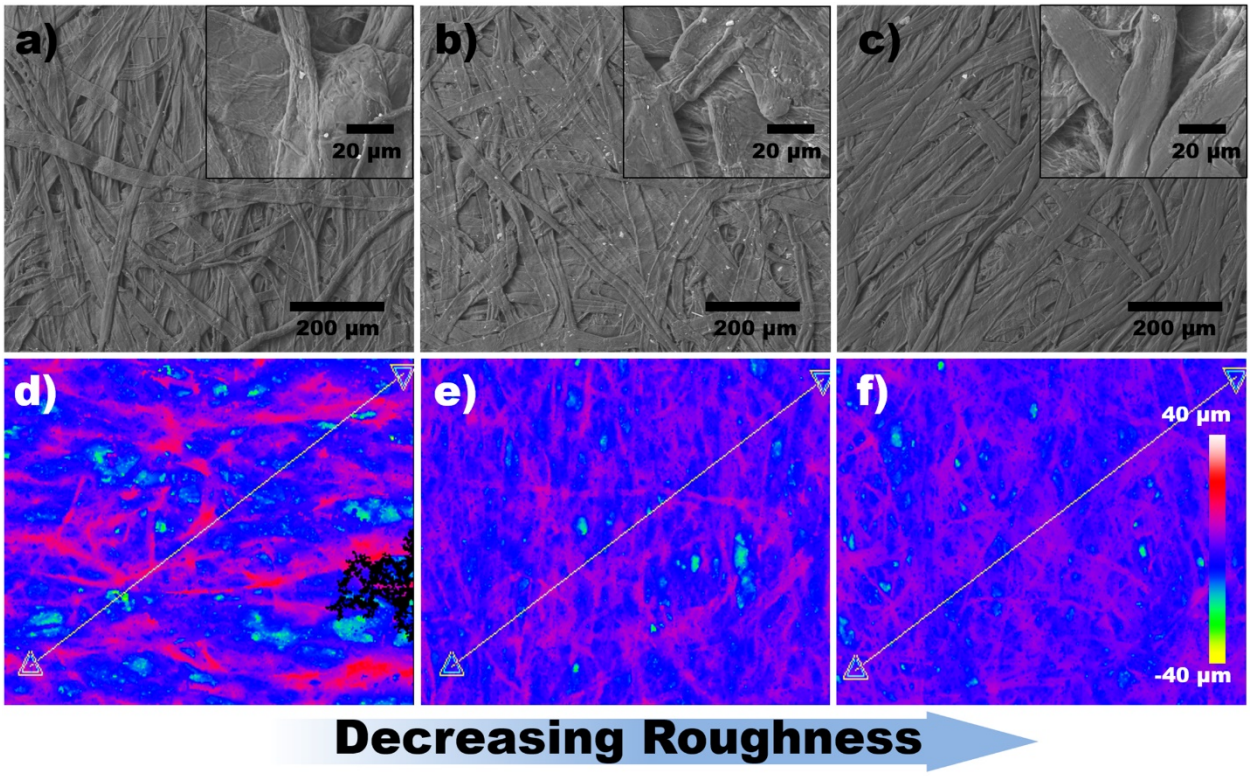

Figure 2. Topology of cellulose substrates. a-c) Scanning electron micrographs of Paper I, II, and III. d-f) Surface profilometry of Paper I, II, and III. The diagonal lines represent the location of the 2D profile.

4. Results and Discussion

Three paper substrates (Paper I, Paper II, and Paper III) differing in degrees of calendaring were used with and without chemisorbed fluoroalkylsilanes. Roughness of the paper substrates decreased with increasing calendering pressure or number of passes through the rollers. **Figure 2** shows changes in surface topology of calendered substrates, with Paper I having the largest roughness (Swedish height, H = 24.7 ± 2.8 µm), followed by II (H = 14.8 ± 1.0 µm), and III (H = 11.6 ± 2.2 µm). Details of Swedish height measurements are provided in the methods section. The untreated samples remained hydrophilic as demonstrated by wicking of water, but become ultra-hydrophobic (contact angles 130-140°) upon treatment with fluoroalkylsilanes as previously demonstrated.[17]

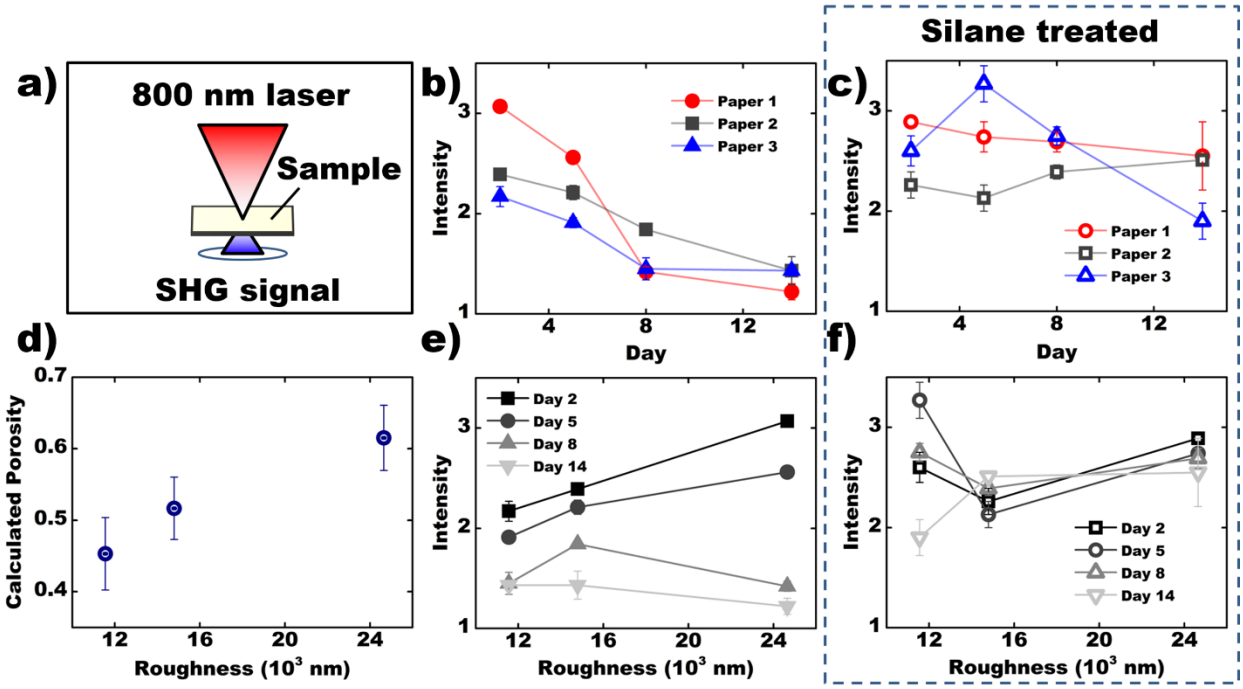

Figure 3. a) Schematic of second-harmonic generation (SHG) imaging. Normalized collagen intensity as a function of time for b) untreated and c) silane treated paper. d) Calculated porosity for paper substrates with varied degree of calendering. Normalized collagen intensity as a function of roughness for e) untreated and f) silane treated paper.

4.1 Effect of surface properties on amount of adsorbed collagen

Collagen secretion by NIH/3T3 fibroblasts cultured on the paper substrates were observed using SHG microscopy in transmission mode (**Figure 3a**). This technique selectively detects surface adsorbed collagen because free fiber bundles will be stochastically distributed in the CM. Collagen intensities were normalized to unseeded cellulose and glass substrates, incubated for the same duration in the CM. This signal was also compared to quantified DNA measured after lysing the cells present on the substrates, which showed similar trend with the data in given in **Figure 3**.

Collagen intensity of all paper substrates decreased over time (**Figure 3b**) with concomitant loss of structural integrity of untreated paper. We infer that metabolism and related cellular exudates is likely degrading the paper, hence, releasing surface adsorbed collagen into the media. Cells attached to the substrate could also participate in collagenase activity leading to collagen signal loss, however, such influence requisite significant cell contractility, which is highly unlikely given their limited adhesion with cellulose.[41, 42] We subsequently treated the paper substrates with fluorinated alkyl silanes to improve stability during cell culture, which has been shown to delay biodegradation, in part, due to restricted permeation of moisture.[10] As expected, the dependence of collagen intensity with time diminished on treated paper (**Figure 3c**). Paper III showed fluctuations but nonetheless always retained higher adsorbed collagen than its untreated counterpart.

Paper is widely regarded as a 3D cell culture platform due to its porous nature that could potentially host cells throughout the thickness of the material (**Figure 3d**).[12] This is evident through the initially linear relationship between collagen intensity and substrate roughness or porosity (**Figure 3e**). After a prolonged period (>8 days), degradation of the substrate leads to a decrease in capacity to support collagen. The initial rate of degradation also increased with

roughness (**Figure 3e**), presumably due to greater inter-fiber bonding created in calendered samples.

The silane treated hydrophobic paper substrates showed no consistent correlation between intensity and roughness (porosity) (**Figure 3f**), indicating that collagen is concentrated at the surface rather than residing within pores of the substrate. Among treated paper, however, rougher substrates (Paper I and II) showed greater stability in collagen adsorption over 14 days compared to the smoother Paper III. We infer that this observation arises from poor collagen adhesion in smooth surfaces. The surface energy mismatch with collagen was verified using glass substrates, which demonstrated significantly lower intensities after silanization (**Figure 4a**).

Additionally, swelling measurements using cell culture media (CM) on the cellulose substrates uncover that both untreated and treated papers have statistically similar values (**Figure 4b-c**). This verifies that as expected,[10] a significant amount of water is absorbed into the fibers of both substrates. Thus, the differences collagen intensity is not an effect of CM transport into the substrates.

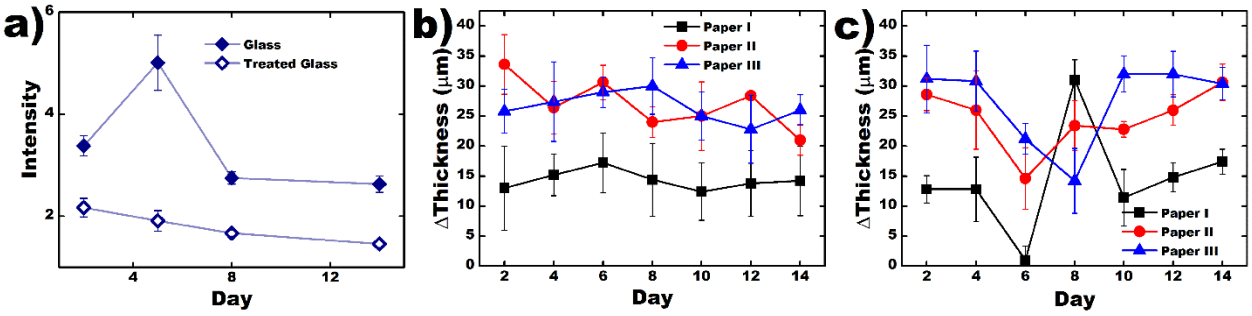

Figure 4. a) Normalized collagen intensity in cultured glass substrates. Glass coverslips are included as a control substrate with smooth surface (H = 6 ± 3 nm). Silane treatment lowered the hydrophilicity of the glass with water contact angles changing from *ca* 20° to 86°. Change in thickness after exposing in cell culture media as a function of time of b) pristine and c) alkyl silane treated cellulose.

4.2 Effect of surface properties on collagen orientation

Since the fabricated paper has a bias in fiber orientation, we hypothesize that a combination of surface properties and fiber orientation can affect organization of adsorbed collagen. Collagen organization facilitates different applications from being highly aligned in scar tissues and keloids, to more disordered in natural dermis.[43, 44] Thus, the ability to control collagen alignment could substantially improve the applicability of paper (or analogous fibrous materials) in tissue engineering. **Figure 5** shows the heat maps of collagen organization on each paper substrate on day 14. Here, samples were imaged from 0 to 360° and the resulting region of interests (ROIs) were fit using Equation 1. Empty ROIs indicate that collagen was not detected. The resulting angles were color coded to help visualize regions of organization. For example, the lines in untreated paper I, II and treated paper III have highly mixed colors, indicating a disorganized collagen pattern. Conversely, treated paper I, II and untreated paper III have more uniform colors, indicating that there are large regions of organization. The angles in these orientation maps were plotted as a histogram and fit using a Gaussian. It should be noted that the 2D maps presented here represent an average orientation through the path of the beam, meaning that multilayered collagen fibers and multilevel stacked (in the case of the 3D untreated paper) are taken into account.

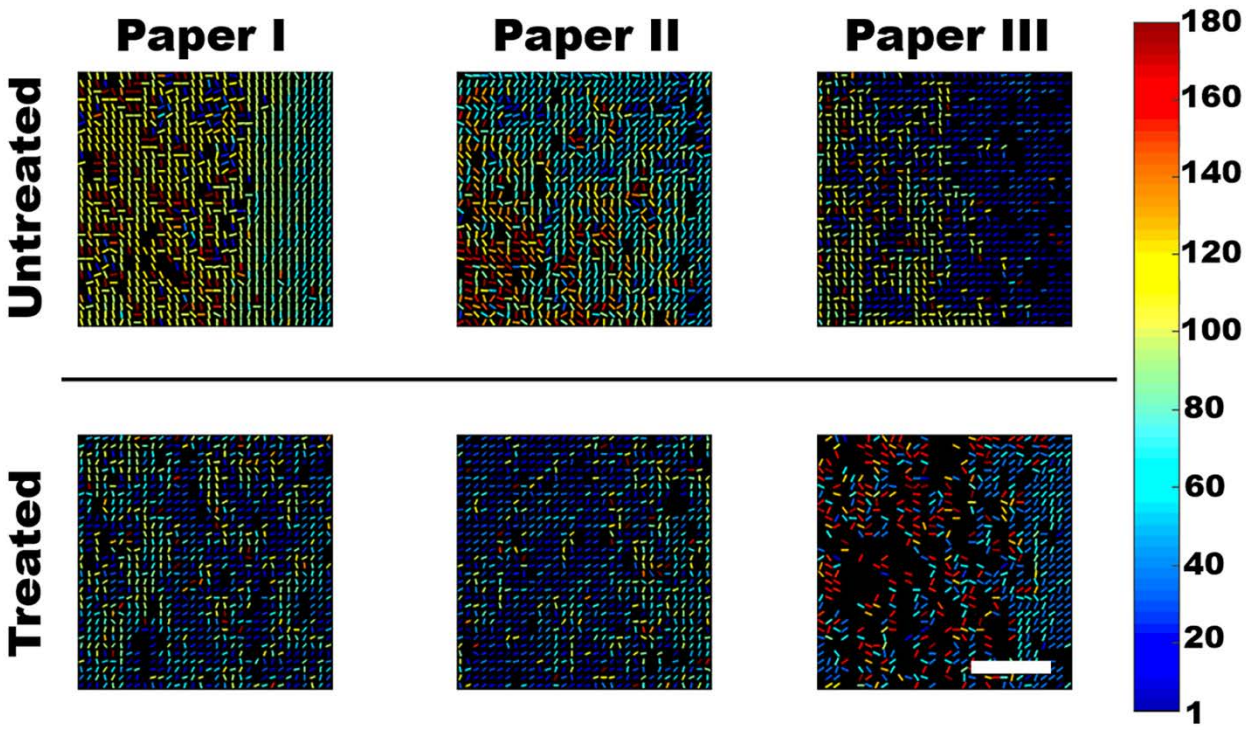

Figure 5. Heat map illustrating collagen organization on paper substrate on day 14. Lines are placed in region of interests (ROIs) in which collagen was detected and the colors represent the collagen orientation. The legend for the heat map provided on the right indicates angle in degrees. Scale bar = 50μm.

Orientation of collagen was quantified using full width at half-maximum (FWHM) of histograms generated using the signals in **Figure 5**. All substrates (untreated and treated) initiated (Day 2) with a small FWHM (**Figure 6a-b),** indicating organized collagen. Data points at longer periods were plotted relative to this initial value (ΔFWHM) to probe the change in organization over time. Collagen organization showed insignificant changes for the untreated samples over the initial 8 days of culture ($p < 0.05$) (**Figure 6a**), however, upon extended culture time, degradation of the paper led to disorganized collagen. Control experiments reveal that degradation is induced by interactions between the substrate and cellular exudates since the culture media by itself did not

lead to observable degradation. Interestingly, the change in collagen organization is almost identical to the trend displayed by change in collagen intensity (**Figure 6c-d**), signifying a relationship between collagen loss and disorder. We infer that the decrease in collagen intensity and order occurs simultaneously due to conceding influence from the substrate, which could also originate from degradation or poor cell-matrix interactions.

Higher statistical moments (skewness and kurtosis) of the Gaussian fits to the collagen organization histograms were used to verify the influence of the substrates (**Figure 6e-f**). The decrease in skewness (approaching 0) over time occurs concomitantly with collagen loss and disorganization, verifying the diminishing influence of the substrate on the cells, which is expected to produce stochastically (Gaussian) distributed collagen.

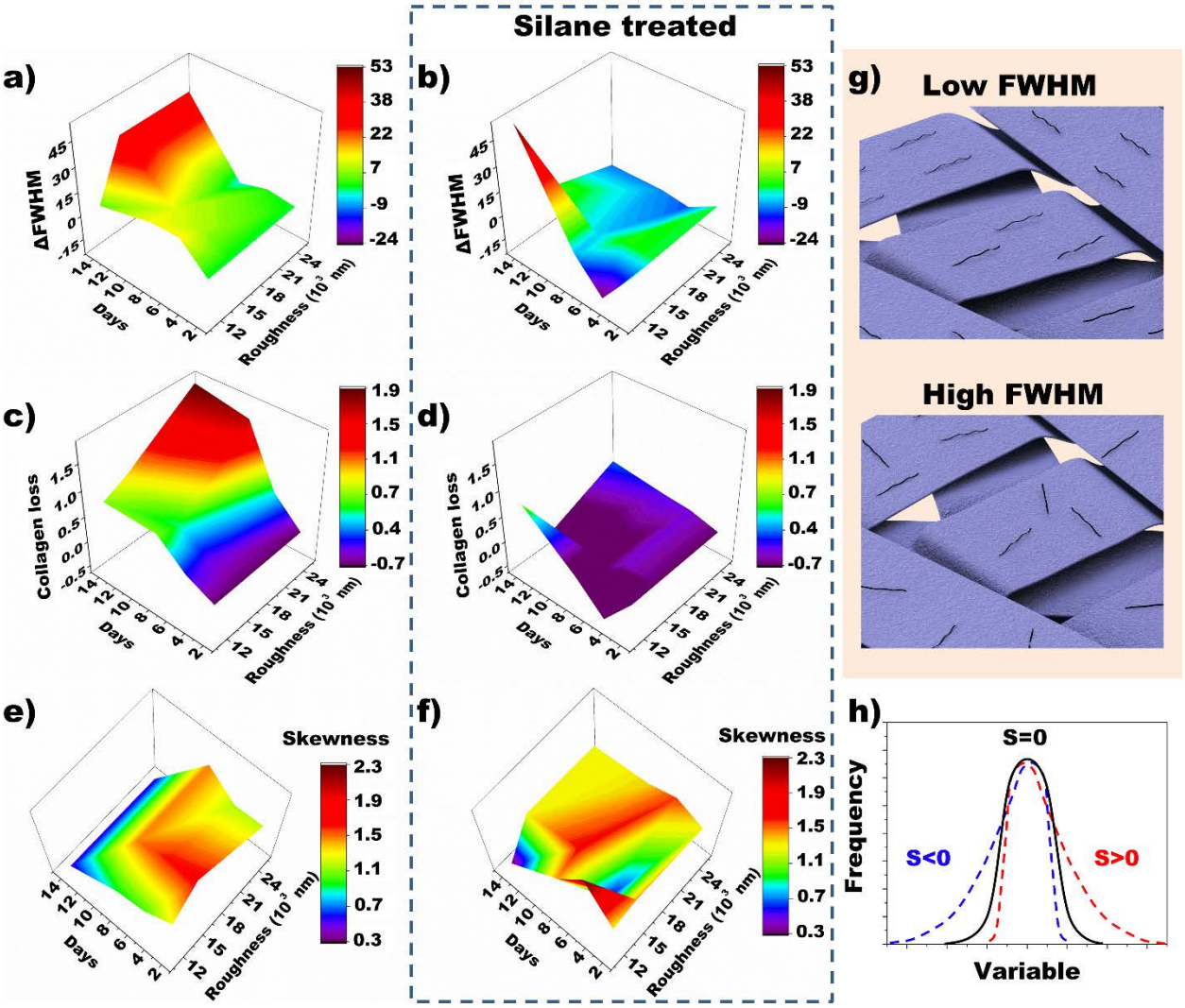

Figure 6. a-b) Change in collagen organization (ΔFWHM), c-d) collagen loss and e-f) skewness as a function of time and roughness on untreated and treated paper substrates. g) Relationship between FWHM and collagen organization. h) Graphical representation of skewness.

4.3 Transition from bulk to surface dominated substrate

The lack of correlation between collagen intensity and porosity in hydrophobic paper indicates that the substrate transitions from a 3D to 2D-like cell culture platform. In this case, the "effective surface" is now at the interface between the hydrophobic paper substrate and culture media, which does not include the buried cellulose fibers. This finding implies that cell culture

using hydrophobic paper should not be directly compared with ordinary paper because 2D scaffolds are well known to produce dissimilar cell biology and morphology.[4, 45, 46]

Amongst the 2D-like hydrophobic substrates, we observed that smoother paper (Paper III) exhibits significant fluctuations in collagen intensity and organization (**Figure 3c** & **Figure 6b**). On the other hand, these fluctuations were not observed in analogous rougher substrates (Paper I & II) suggesting a roughness (porosity)-chemistry interplay in collagen adsorption. This is further verified by comparing a known smooth 2D substrate (glass coverslips), which also showed fluctuations in collagen intensity over time (**Figure 4a**). We therefore infer that mechanical trapping, interfacial energy matching, and fiber direction affects the overall collagen adsorption.

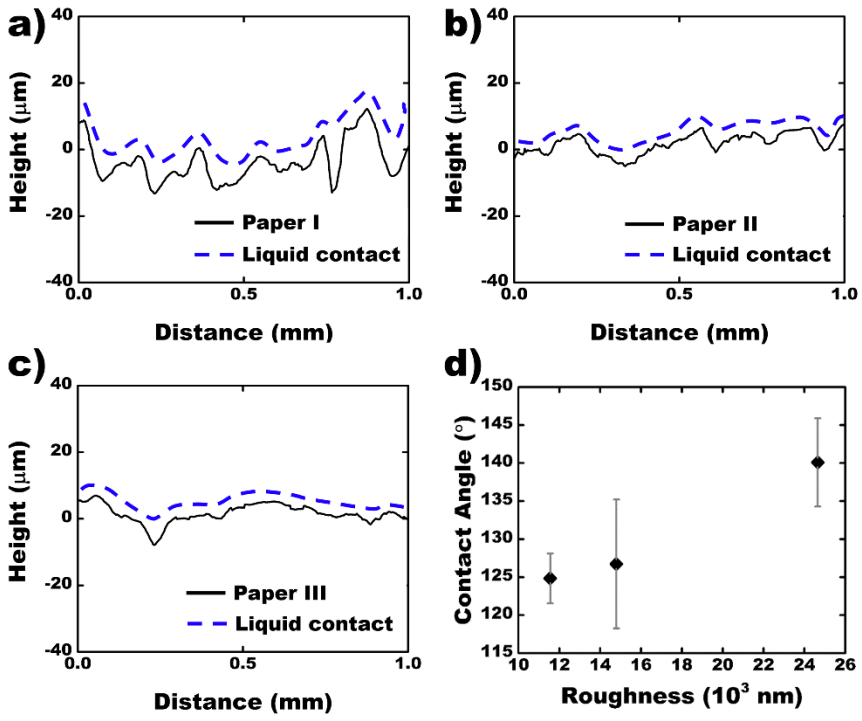

Figure 7. Two-dimensional profile of substrate with estimated liquid contact on hydrophobic surface.

The uneven surfaces in Paper I could lead to capillary driven Cassie-Baxter type CM pinning—the petal effect **(Figure 7a-c).**[47] This is further supported by water contact angle

measurements (**Figure 7d**) whereby Paper I showed the highest water contact angle (140°), followed by Paper II and III (~130° each, Paper II showing higher standard deviation). Considering Cassie's law for heterogeneous surfaces, $\cos(\theta^*) = rf\cos(\theta) + f - 1$, the apparent contact angle (θ*) increases with roughness (r) and fraction of wetted surface (*f*).[48] We, therefore, demonstrate control over these parameters in paper through a simple processes of shearing-driven fiber organization, calendaring and surface modification. By using a rougher substrate, and match in interfacial surface energy, we demonstrate improvement in surface adhesion of collagen, hence, stability of collagen organization.

5. Conclusions

In conclusions, we demonstrate that the secondary structures in paper significantly affect cellular microenvironment, hence, collagen secretion by NIH/3T3 fibroblast cells. Furthermore, these responses are also found to be coupled with wetting properties of paper. Specifically, we conclude that:

i) Paper effectively provides a 3D scaffold for cell culture, but performance is highly time dependent and can be controlled by changing porosity.

ii) Treatment with fluorinated alkyl silane renders paper hydrophobic and significantly improves substrate stability during cell culture, however, transitions from a 3D to 2D-like scaffold.

iii) Hydrophobic paper with higher roughness shows improved collagen adsorption, hence, the ability to host collagen becomes dominated by pinning at the surface due to the petal effect.

iv) The influence of the paper substrate on its capacity to host collagen simultaneously affects collagen organization.

Acknowledgements

This research was supported by start-up funding from Iowa State University and a Black and Veatch faculty fellowship to M.T. We thank the European Synchrotron Radiation Facility (ESRF), Grenoble, for tomography imaging. The authors would also like to thank Dr. Warren Straszheim (SEM) and Dr. Mark Placette (profilometer) for technical assistance.

References

[1] M. Tommila, A. Jokilammi, R. Penttinen, E. Ekholm, Cellulose- a biomaterial with cell-guiding property, in, InTech, 2013, pp. 83-104.
[2] M. Cotterell, The terracotta warriors: the secret codes of the emperor's army, Bear & Co, Rochester, Vt, 2004.
[3] A.A. Silva, Molecular weight distribution analysis of wood pulp cellulose by size exclusion chromatography, in, 1995.
[4] D.J. Modulevsky, C. Lefebvre, K. Haase, Z. Al-Rekabi, A.E. Pelling, Apple derived cellulose scaffolds for 3D mammalian cell culture, PLoS One, 9 (2014) e97835/97831-e97835/97810, 97810 pp.
[5] M. Bhattacharya, M.M. Malinen, P. Lauren, Y.-R. Lou, S.W. Kuisma, L. Kanninen, M. Lille, A. Corlu, C. GuGuen-Guillouzo, O. Ikkala, A. Laukkanen, A. Urtti, M. Yliperttula, Nanofibrillar cellulose hydrogel promotes three-dimensional liver cell culture, Journal of Controlled Release, 164 (2012) 291-298.
[6] A. Svensson, E. Nicklasson, T. Harrah, B. Panilaitis, D.L. Kaplan, M. Brittberg, P. Gatenholm, Bacterial cellulose as a potential scaffold for tissue engineering of cartilage, Biomaterials, 26 (2005) 419-431.
[7] S. Birkheur, P.C.d.S. Faria-Tischer, C.A. Tischer, E.F. Pimentel, M. Fronza, D.C. Endringer, A.P. Butera, R.M. Ribeiro-Viana, Enhancement of fibroblast growing on the mannosylated surface of cellulose membranes, Mater. Sci. Eng., C, 77 (2017) 672-679.
[8] R. Derda, A. Laromaine, A. Mammoto, S.K.Y. Tang, T. Mammoto, D.E. Ingber, G.M. Whitesides, Paper-supported 3D cell culture for tissue-based bioassays, Proceedings of the National Academy of Sciences, 106 (2009) 18457.
[9] S.-H. Kim, H.R. Lee, S.J. Yu, M.-E. Han, D.Y. Lee, S.Y. Kim, H.-J. Ahn, M.-J. Han, T.-I. Lee, T.-S. Kim, S.K. Kwon, S.G. Im, N.S. Hwang, Hydrogel-laden paper scaffold system for origami-based tissue engineering, Proc. Natl. Acad. Sci. U. S. A., 112 (2015) 15426-15431.
[10] S. Oyola-Reynoso, D. Kihereko, B.S. Chang, J.N. Mwangi, J. Halbertsma-Black, J.-F. Bloch, M.M. Thuo, M.M. Nganga, Substituting Plastic Casings with Hydrophobic (Perfluorosilane treated) paper improves Biodegradability of Low-Cost Diagnostic Devices, Ind. Crops Prod., 94 (2016) 294-298.

[11] H.-J. Park, S.J. Yu, K. Yang, Y. Jin, A.-N. Cho, J. Kim, B. Lee, H.S. Yang, S.G. Im, S.-W. Cho, Paper-based bioactive scaffolds for stem cell-mediated bone tissue engineering, Biomaterials, 35 (2014) 9811-9823.
[12] K. Ng, B. Gao, K.W. Yong, Y. Li, M. Shi, X. Zhao, Z. Li, X. Zhang, B. Pingguan-Murphy, H. Yang, F. Xu, Paper-based cell culture platform and its emerging biomedical applications, Mater. Today (Oxford, U. K.), 20 (2017) 32-44.
[13] D.C. Christodouleas, F.C. Simeone, A. Tayi, S. Targ, J.C. Weaver, K. Jayaram, M.T. Fernández-Abedul, G.M. Whitesides, Fabrication of Paper-Templated Structures of Noble Metals, Advanced Materials Technologies, 2 (2017) 1600229.
[14] P.R. Gregory, A. Martin, B.S. Chang, S. Oyola-Reynoso, J.-F. Bloch, M.M. Thuo, Inverting Thermal Degradation (iTD) of Paper Using Chemi- and Physi-Sorbed Modifiers for Templated Material Synthesis, Frontiers in Chemistry, 6 (2018).
[15] D. Akilbekova, K.M. Bratlie, Quantitative characterization of collagen in the fibrotic capsule surrounding implanted polymeric microparticles through second harmonic generation imaging, PLoS One, 10 (2015) e0130386/0130381-e0130386/0130317.
[16] S. Oyola-Reynoso, C. Frankiewicz, B. Chang, J. Chen, M.M. Thuo, J.F. Bloch, Paper-based microfluidic devices by asymmetric calendaring, Biomicrofluidics, 11 (2017) 014104.
[17] S. Oyola-Reynoso, I.D. Tevis, J. Chen, B.S. Chang, S. Cinar, J.F. Bloch, M.M. Thuo, Recruiting Physisorbed Water in Surface Polymerization for Bio- Inspired Materials of Tunable Hydrophobicity, J. Mater. Chem. A, 4 (2016) 14729-14738.
[18] P. Vernhes, J.-F. Bloch, A. Blayo, B. Pineaux, Effect of calendering on paper surface micro-structure: A multi-scale analysis, Journal of Materials Processing Technology, 209 (2009) 5204-5210.
[19] P. Vernhes, M. Dubé, J.F. Bloch, Effect of calendering on paper surface properties, Applied Surface Science, 256 (2010) 6923-6927.
[20] S.R. du Roscoat, M. Decain, X. Thibault, C. Geindreau, J.F. Bloch, Estimation of microstructural properties from synchrotron X-ray microtomography and determination of the REV in paper materials, Acta Materialia, 55 (2007) 2841-2850.
[21] C.M. Ali, B. Jean-Francis, B. Elodie, M. Patrice, 3D synchrotron X-ray microtomography for paper structure characterization of z-structured paper by introducing micro nanofibrillated cellulose, Nordic Pulp & Paper Research Journal, 31 (2016).
[22] F.J. Ávila, O. del Barco, J.M. Bueno, Quantifying External and Internal Collagen Organization from Stokes-Vector-based Second Harmonic Generation Imaging Polarimetry, Journal of Optics, 19 (2017) 105301.
[23] S. Roth, I. Freund, Second harmonic generation in collagen, The Journal of Chemical Physics, 70 (1979) 1637-1643.
[24] P.C. Stoller, P.M. Celliers, K.M. Reiser, A.M. Rubenchik, Imaging collagen orientation using polarization-modulated second harmonic generation, Proc. SPIE-Int. Soc. Opt. Eng., 4620 (2002) 157-165.
[25] T. Yasui, Y. Tohno, T. Araki, Characterization of collagen orientation in human dermis by two-dimensional second-harmonic-generation polarimetry, J. Biomed. Opt., 9 (2004) 259-264.
[26] O. Schmut, The organization of tissues of the eye by different collagen types, Albrecht von Graefes Arch. Klin. Exp. Ophthalmol., 207 (1978) 189-199.
[27] P.P. Provenzano, K.W. Eliceiri, J.M. Campbell, D.R. Inman, J.G. White, P.J. Keely, Collagen reorganization at the tumor-stromal interface facilitates local invasion, BMC Med., 4 (2006) No pp. given.
[28] K. Esbona, Y. Yi, S. Saha, M. Yu, R.R. Van Doorn, M.W. Conklin, D.S. Graham, K.B. Wisinski, S.M. Ponik, K.W. Eliceiri, L.G. Wilke, P.J. Keely, The Presence of Cyclooxygenase 2, Tumor-Associated Macrophages, and Collagen Alignment as Prognostic Markers for Invasive Breast Carcinoma Patients, The American Journal of Pathology, 188 (2018) 559-573.
[29] B. Krishnamachary, I. Stasinopoulos, S. Kakkad, M.-F. Penet, D. Jacob, F. Wildes, Y. Mironchik, A.P. Pathak, M. Solaiyappan, Z.M. Bhujwalla, M.-F. Penet, A.P. Pathak, Z.M. Bhujwalla, Breast cancer cell cyclooxygenase-2 expression alters extracellular matrix structure and function and numbers of cancer associated fibroblasts, Oncotarget, 8 (2017) 17981-17994.

[30] A. Keikhosravi, J.S. Bredfeldt, A.K. Sagar, K.W. Eliceiri, Second-harmonic generation imaging of cancer, Methods Cell Biol, 123 (2014) 531-546.
[31] T. Hompland, A. Erikson, M. Lindgren, T. Lindmo, C. de Lange Davies, Second-harmonic generation in collagen as a potential cancer diagnostic parameter, J. Biomed. Opt., 13 (2008) 054050/054051-054050/054011.
[32] B.K. Brisson, E.A. Mauldin, W. Lei, L.K. Vogel, A.M. Power, A. Lo, D. Dopkin, C. Khanna, R.G. Wells, E. Pure, S.W. Volk, Type III Collagen Directs Stromal Organization and Limits Metastasis in a Murine Model of Breast Cancer, Am. J. Pathol., 185 (2015) 1471-1486.
[33] A. Tenboll, B. Darvish, W. Hou, A.-S. Duwez, S.J. Dixon, H.A. Goldberg, B. Grohe, S. Mittler, Controlled Deposition of Highly Oriented Type I Collagen Mimicking In Vivo Collagen Structures, Langmuir, 26 (2010) 12165-12172.
[34] C.C. Wang, K.C. Yang, K.H. Lin, H.C. Liu, F.H. Lin, A highly organized three-dimensional alginate scaffold for cartilage tissue engineering prepared by microfluidic technology, Biomaterials, 32 (2011) 7118-7126.
[35] W.F. Liu, C.S. Chen, Engineering biomaterials to control cell function, in, 2005.
[36] F. Liu, J.D. Mih, B.S. Shea, A.T. Kho, A.S. Sharif, A.M. Tager, D.J. Tschumperlin, Feedback amplification of fibrosis through matrix stiffening and COX-2 suppression, Journal of Cell Biology, 190 (2010) 693-706.
[37] S. Manara, F. Paolucci, B. Palazzo, M. Marcaccio, E. Foresti, G. Tosi, S. Sabbatini, P. Sabatino, G. Altankov, N. Roveri, Electrochemically-assisted deposition of biomimetic hydroxyapatite-collagen coatings on titanium plate, Inorganica Chimica Acta, 361 (2008) 1634-1645.
[38] J. Lincks, B.D. Boyan, C.R. Blanchard, C.H. Lohmann, Y. Liu, D.L. Cochran, D.D. Dean, Z. Schwartz, Response of MG63 osteoblast-like cells to titanium and titanium alloy is dependent on surface roughness and composition, The Biomaterials: Silver Jubilee Compendium, 19 (2006) 147-160.
[39] G. Bhardwaj, T.J. Webster, Increased NIH 3T3 fibroblast functions on cell culture dishes which mimic the nanometer fibers of natural tissues, Int. J. Nanomed., 10 (2015) 5293-5299.
[40] G. Camci-Unal, A. Laromaine, E. Hong, R. Derda, G.M. Whitesides, Biomineralization Guided by Paper Templates, Scientific Reports, 6 (2016) 27693-27693.
[41] J. Wang, A. Boddupalli, J. Koelbl, D.H. Nam, X. Ge, K.M. Bratlie, I.C. Schneider, Degradation and Remodeling of Epitaxially Grown Collagen Fibrils, Cellular and Molecular Bioengineering, 12 (2019) 69-84.
[42] R. Malik, P.I. Lelkes, E. Cukierman, Biomechanical and biochemical remodeling of stromal extracellular matrix in cancer, Trends in Biotechnology, 33 (2015) 230-236.
[43] D.H.M. Verhaegen Pauline, P.M. Van Zuijlen Paul, M. Pennings Noor, J. Van Marle, B. Niessen Frank, M.A.M. Van Der Horst Chantal, E. Middelkoop, Differences in collagen architecture between keloid, hypertrophic scar, normotrophic scar, and normal skin: An objective histopathological analysis, Wound Repair and Regeneration, 17 (2009) 649-656.
[44] D.H.M. Verhaegen Pauline, J.A.N. Van Marle, A. Kuehne, J. Schouten Hennie, A. Gaffney Eamonn, K. Maini Philip, E. Middelkoop, P.M. Van Zuijlen Paul, Collagen bundle morphometry in skin and scar tissue: a novel distance mapping method provides superior measurements compared to Fourier analysis, Journal of Microscopy, 245 (2011) 82-89.
[45] B.M. Baker, C.S. Chen, Deconstructing the third dimension – how 3D culture microenvironments alter cellular cues, Journal of Cell Science, 125 (2012) 3015.
[46] L. Pastorino, E. Dellacasa, S. Scaglione, M. Giulianelli, F. Sbrana, M. Vassalli, C. Ruggiero, Oriented collagen nanocoatings for tissue engineering, Colloids and Surfaces B: Biointerfaces, 114 (2014) 372-378.
[47] L. Feng, Y. Zhang, J. Xi, Y. Zhu, N. Wang, F. Xia, L. Jiang, Petal Effect: A Superhydrophobic State with High Adhesive Force, Langmuir, 24 (2008) 4114-4119.
[48] A. Marmur, Wetting on Hydrophobic Rough Surfaces: To Be Heterogeneous or Not To Be?, Langmuir, 19 (2003) 8343-8348.